INTERNATIONAL JOURNAL OF INNOVATIVE RESEARCH IN MULTIDISCIPLINARY EDUCATION

ISSN (print): 2833-4515, ISSN (online): 2833-4531

Volume 05 Issue 03 March 2026

DOI: 10.58806/ijirme.2026.v5i3n05 Impact factor- 7.614

Page No. 207-218

Image Processing Approaches for AI-Driven Classification and Anomaly Detection of IES Light Distribution Patterns

Dr. Kawther H. Al-khafaji

Assist. Prof., Faculty of Education for Woman, University of Kufa, Iraq.

ABSTRACT: This study describes an image-based approach to examining photometric feature values of IES pattern of light, which are intended to enable AI-based classification and anomaly detection. A complete suite of descriptors: geometric and spatial, uniformity and distribution, statistical shape, beam, texture indices, and falloff of intensity of high-quality light were obtained and meaningfully compared across various lighting setup. The findings indicate that ellipticity, center shift, entropy, skewness, kurtosis, beam width, and GLCM-based texture measurements are good discriminators, which allow distinguishing between focused sources (e.g., Star-Focused, XArrow) and ambient ones (e.g., Bollard, Display). Combining all these complementary characterizations, the proposed framework provides a holistic system of photometric analysis to enhance the accuracy of the automated classification and deliver useful information in finding anomaly and application-specific optimization in a lighting design. All the feature extraction, processing, and comparative analysis were done in MATLAB which provides reproducible and computationally efficient features. The results were complemented with texture based GLCM features which have StarFocused features and high energy and homogeneity, defined features which have high contrast, and always good value of correlation with all patterns connotations of structural regularity.

KEYWORDS: Image Processing, AI, IES Light Distribution Patterns, Photometric Analysis, Pattern Recognition, Image-based photometry, Light pattern analysis, Photometric features, GLCM, Computer vision, Anomaly detection, Indoor lighting, Computer vision.

1. INTRODUCTION

The Illuminating Engineering Society (IES) has developed a standardized form of description of the distribution of light by luminaires, called the IES photometric file. These files include quantitative data including luminous intensity values, beam angles, and photometric distribution, which could be represented as IES light patterns. These patterns are the dispersal patterns of light in space either concentrated in a small area, diffused in a wide area as a flood or asymmetrical diffusion of light either to roadways or to buildings. The critical role of indoor lighting in the formation of visual comfort, task performance, and spatial perception is due to the fact that many lighting studies highlight the close connection between the quality of illumination and the performance of humans. IES files describe how light from a lamp is distributed in a room. This data is provided by many manufacturers so that lighting designers can realistically simulate how a project will look when a specific light source is used. 3D artists also use this data to calculate their images more realistically [1,2]

The objective of lighting estimation is to reconstruct lighting of a single image of limited field of view. It has numerous applications in many computer vision and computer graphics problems like high-dynamic-range (HDR) relighting in mixed reality, etc. Nevertheless, the estimation of lighting is an under constrained task because it seeks to reconstruct the 360-degree full view light map of an image with a narrow field of view. Moreover, high-dynamic-range (HDR) lighting must be reconstructed on the basis of low-dynamic-range (LDR) measurements to be used to relight objects realistically. The level of light influences the way people engage with the surrounding, which impacts productivity, safety, and psychological health. The classic photometric assessment is based on the physical measurements of the illuminance, beam angle, and homogeneity, which are usually measured with special equipment, such as lux meters and goniophotometers. Although these instruments are precise, they are usually costly, need controlled laboratory conditions, and are not commonly available in the teaching, building, and small-scale engineering environments [3]. Image-based photometric analysis has become an alternative to the widely used photometric analysis with the fast development of digital imaging and computer vision. Digital cameras of high resolution are able to record finer illumination patterns so that geometric and photometric characteristics can be directly extracted out of images based on a set of photometric properties that characterize the intensity, distribution and direction of light [4].

This is less expensive, more accessible and can be analyzed automatically without special hardware. Current studies on illumination estimation prove the usefulness of image-based illumination estimation techniques in extracting lighting features of single or multi-images [5].

Recent studies have covered the estimation of image-based illumination, hotspots, and beam spread. Nevertheless, there have been few studies on applying artificial intelligence (AI) to classify light patterns and identify illumination anomalies. These anomalies can be anomalous beam shapes, abnormal light distributions, unforeseen hotspots, or deviation of photometric behavior. These patterns are important to quality control, optimization of lighting design, and automated inspection systems. The latest AI-based anomaly detection models exhibit high abilities to detect abnormal patterns in visual information in both industrial and optical scenarios [6,7,8].

This paper develops a new AI-based system of classifying light patterns and detecting anomalies based on image-based photometric characteristics. The technique derives a rich set of illumination features such as beam radius, uniformity ratio, hotspots density, radial intensity slope, heatmap entropy, radiative distribution, gradients, texture patterns (GLCM), spot shape, and beam angle to learn machine learning models that can discriminate between normal and abnormal illumination patterns with great accuracy. The solution suggested is low-cost, scalable, and automated way of evaluating the set of indoor lighting systems through integrating the newest digital image processing techniques with the use of smart learning algorithms. This allows a small portion of light knowledge that borders the actual physical analysis yet is more effective and faster and the skeleton is of colossal importance in use in architecture, manufacturing, education, optical investigation and intelligent building technologies.

2. BACKGROUND

Traditional lighting analysis method is by photometric measurements which determine performance of the light in a physical setting. Some of the important parameters include illuminance, luminous intensity, beam angle and uniformity. These will be some of the measures that will test the lighting standards. The physical measurement tools are not however always possible in large scale or automated measurement [9,10]. Image based photometry has also been thought of to be of interest as a more flexible and less expensive one. Through the distribution of pixel intensities, scientists can estimate the patterns of illumination patterns, identify hotspots, and measure uniformity. Some of the techniques that have been extensively applied in order to obtain large photometric information on images are the thresholding, edge discovering and radial profiling[7]. The possibilities of image-based analysis have been increased in recent times due to artificial intelligence. Patterns categories, anomalies and learning multifaceted relationships between photometric features can be categorized using machine learning models. One of the areas where AI can be used to execute automated inspection, smart lighting and quality control may be lighting. Nonetheless, AI application and photometric feature extraction have not been well studied especially on indoor spotlights analysis[11,12]. This gap is filled in by the work that integrates image processing and AI-based classification and anomaly detection and provides a new form of automated light analysis [11].

3. MATHEMATICAL MODEL

The mathematical representation of the suggested AI propelled analysis of lighting is built on two principal parts:

1. **Photometric feature extraction from digital images**
2. **Machine learning - based classification and anomaly detection**

These components work together to convert raw illumination images into quantitative descriptors and then into intelligent decisions. [12]

3.1 Photometric Feature Extraction

Given a grayscale illumination image ($G(x, y)$), several photometric descriptors are computed to characterize the light pattern.

3.1.1 Beam Radius

The illuminated region is segmented using thresholding, and the equivalent radius is computed as:

$$r = \frac{\mathrm{D_{eq}}}{2} \qquad (1)$$

Where; D_{eq} is the equivalent diameter of the segmented region.

3.1.2 Radial Intensity Profile

The radial distance of each pixel from the centroid (c_x, c_y) is:

$$R(x, y) = \sqrt{(x - c_x)^2 + \left(y - c_y\right)^2} \qquad (2)$$

The average intensity at radius (r) is:

$$I(r) = \frac{1}{N_r} \sum_{(x,y)\in r} G(x, y) \qquad (3)$$

Where; (N_r) is the number of pixels in the radial bin.

3.1.3 Uniformity Ratio

Uniformity is computed as:

$$U_0 = \frac{E_{min}}{E_{avg}} \qquad (4)$$

Where; (E_{min}): minimum pixel intensity, (E_{avg}): average pixel intensity.

3.1.4 Hotspot Density

A hotspot is defined as any pixel with intensity above a threshold (T_h):

$$T_h = \mu + k \qquad (5)$$

Where;(μ) and (σ) are the mean and standard deviation of pixel intensities. The Hotspot density:

$$H_d = \frac{N_{hot}}{N_{total}} \qquad (6)$$

3.1.5 Heatmap Entropy

Entropy measures illumination randomness:

$$H = -\sum_{i=1}^{L} p_i \log_2(p_i) \qquad (7)$$

Where;(p_i) is the probability of intensity level (i).

3.2 Machine Learning Model (AI Model Description)

Let the feature vector be:

$$F = [r, U_0, H_d, H, s_1, s_2, \ldots, s_n] \qquad (8)$$

Where;

r : beam radius

U_0 : uniformity ratio

H_d : hotspot density

H : heatmap entropy

s_i: slope values from the radial intensity profile

These features capture the shape, distribution, and structure of the illumination pattern.

3.2.1 Classification Model

A classifier (C) maps features to lighting categories:

$$\hat{y} = C(\mathrm{F}) \qquad (9)$$

Where ($\hat{y}$) is the predicted lighting class.

The following sections present two illustrative diagrams: the first outlines the possible classes of light patterns, while the second highlights suitable classifiers commonly applied in machine learning to categorize these patterns.

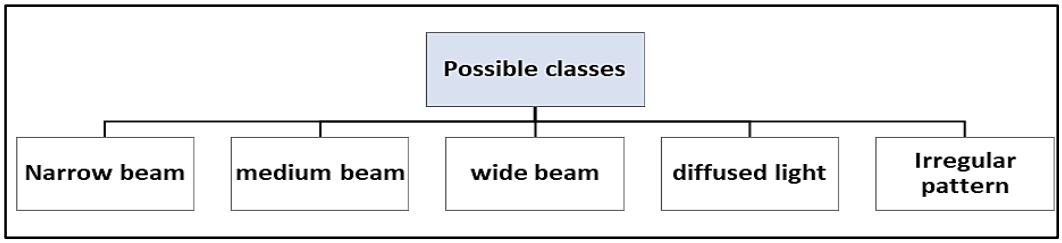


Fig (1): Possible Light Pattern Classes

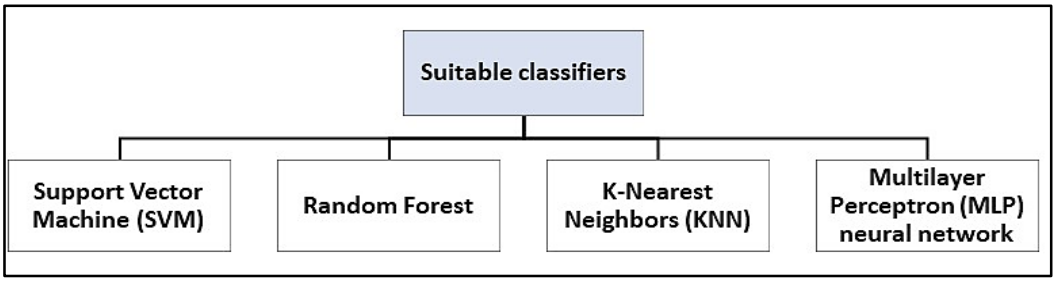


Fig (2): Suitable Machine Learning Classifiers

3.2.2 Anomaly Detection Model

An anomaly detector (A) identifies abnormal illumination:

$$a = A(F) \qquad (10)$$

Where;

$$a = \begin{cases} 1, & \text{if anomaly detected} \\ 0, & \text{otherwise} \end{cases}$$

4. AI DRIVEN LIGHT PATTERN CLASSIFICATION AND ANOMALY DETECTION ALGORITHM

An algorithm will be applied to the pre-processed digital image in order to extract lighting features and detect anomalies. The output will return the corresponding lighting class label together with an anomaly flag to highlight abnormal cases.

Step 1: Image Preprocessing

1. Load the input image (I).
2. Convert the image in to grayscale: [$G = \text{rgb2gray}(I)$]
3. Apply Gaussian filtering to reduce noise.
4. Normalize pixel intensities to ([0,1]).

Step 2: Light Region Segmentation

5. Compute Otsu threshold (T).
6. Generate binary mask: [$B = \text{imbinarize}(G, T)$]
7. Fill holes and remove small artifacts.
8. Extract the largest connected component.

Step 3: Geometric Feature Extraction

9. Compute centroid (c_x, c_y).
10. Compute equivalent diameter and radius: [$r = \frac{D_{eq}}{2}$]
11. Compute Center-Shift
12. Compute Ellipticity
13. Compute Beam-Width-Pixels
14. Compute Beam-Angle-deg

Step 4: Photometric Feature Extraction

15. Compute radial intensity profile ($I(r)$).
16. Compute uniformity ratio: [$U_0 = \frac{E_{min}}{E_{avg}}$]
17. Compute hotspot density: [$H_d = \frac{N_{hot}}{N_{total}}$]
18. Compute heatmap entropy: [$H = -\sum p_i \log_2(p_i)$]
19. Compute Max-Intensity
20. Compute Peak-Intensity
21. Compute Shadow-Sharpness
22. Compute Edge-Fall off Mean

Step 5: Feature Vector Construction

23. Construct feature vector: [$F = [r, U_0, H_d, H, s_1, s_2, \ldots]$]
24. Compute Skewness
25. Compute Kurtosis
26. Compute Slope-Radial
27. Compute Symmetry-Radial
28. Compute Falloff

Step 6: Texture Feature Extraction (GLCM)

29. Compute GLCM-Contrast
30. Compute GLCM-Correlation
31. Compute GLCM-Energy
32. Compute GLCM-Homogeneity

Step 7: AI Based Classification

33. Apply trained classifier: [$\hat{y} = C(F)$]

Step 8: Anomaly Detection

34. Apply anomaly detector: [$a = A(F)$]

Step 9: Output

Return lighting class label and anomaly flag.

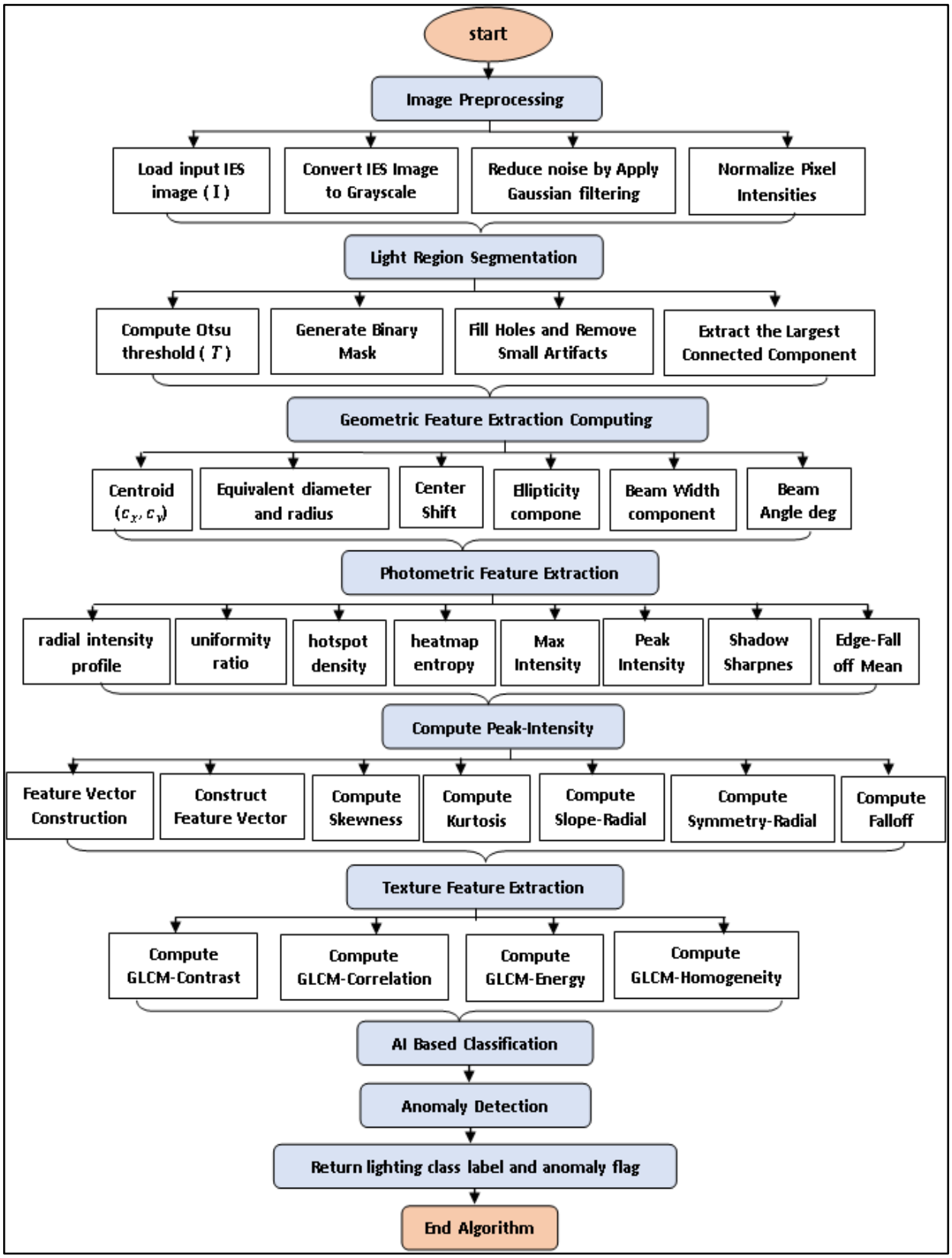


Fig (3) The Flowchart of The Proposed Works

5. THE RESULTS AND DISCUSSION

Table. 1 summarizes the advanced photometric features extracted from the analyzed light patterns. These features capture geometric, statistical, and texture-based properties that are essential for classification and anomaly detection, all the IES image have (800x469) pixel (jpeg type).

Table (1) Advanced Feature Value

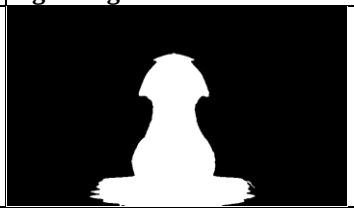
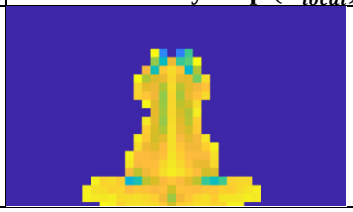
Main Features Summary	The IES image values					
	Display	**vee**	**XArrow**	**StarFocused**	**Defined**	**Bollard**
Radius	141.7632	162.1807	172.9064	85.1795	189.7741	122.5331
Uniformity U_0	0.2451	0.4190	0.4644	0.0000	0.4473	0.5427
Hot spot Density H_d	0.3383	0.3091	0.1942	0.2387	0.2713	0.3981
Entropy H	7.1287	6.5458	6.4270	6.6924	6.8739	5.9617
Skewness	0.3399	0.9007	1.9555	1.3965	0.9578	-0.1902
Kurtosis	1.7633	2.7754	6.4170	4.3932	3.2148	1.8635
Slope Radial	-0.0028	0.0021	0.0014	0.0005	0.0013	0.0000
Symmetry Radial	0.0854	0.0629	0.0515	0.0179	0.0433	0.0076
Falloff	0.3236	-0.1945	-0.1401	-0.0581	-0.1708	-0.0310
Max Intensity	1.0000	1.0000	1.0000	1.0000	1.0000	0.6745
Peak Intensity	1.0000	1.0000	1.0000	1.0000	1.0000	0.6745
Center Shift	222.0859	199.2935	224.3469	172.8316	218.4640	20.3102
Ellipticity	1.4679	1.0599	1.3660	3.6163	1.4611	11.3112
Beam Width Pixels	250.0000	407.0000	194.0000	89.0000	614.0000	769.0000
Beam Angle deg	82.8086	102.8933	58.5846	55.1675	116.5549	144.6477
Shadow Sharpness	0.0987	0.1280	0.0633	0.1106	0.1021	0.1037
Edge Fall off Mean	0.0947	0.1380	0.0620	0.1102	0.1047	0.0891
GLCM Contrast	1.9894	1.5263	1.3173	0.4911	2.0524	1.4294
GLCM Correlation	0.9958	0.9964	0.9950	0.9914	0.9965	0.9935
GLCM Energy	0.6896	0.6068	0.5616	0.8801	0.4875	0.7637
GLCM Homogeneity	0.9567	0.9465	0.9427	0.9813	0.9341	0.9701

It is possible to see a vivid variation in the six light distributions tested (Display, Vee, XArrow, StarFocused, Defined, Bollard). As an example, the Beam Angle values are between narrow beams like StarFocused (55.16) and the wide beams like Bollard (144.65) which represent the variety of optical dispersion. In the same manner, Uniformity (U_0) also varies slightly with StarFocused having the lowest uniformity (0.0000) and Bollard having the highest uniformity (0.5427) that indicates a more uniform flow of light.

Statistical descriptors also point out variations between the patterns. XArrow has a large skewness (1.95) and kurtosis (6.41) which means that the distribution is highly skewed and peaked, whereas Bollard has negative skewness (-0.19) indicating a more balanced intensity distribution. Differences in entropy also indicate the difference in complexity, where Display (7.12) is more informative than Bollard (5.96).

The geometric features like Ellipticity and Center Shift give good indicators of anomaly detection. Bollard is very elliptic (11.31) and has a significantly low center shift (20.31) compared to the overall tendency of other patterns (>170). These outliers indicate that Bollard could be an outlier group, and thus it can be used as an anomaly detector.

GLCM-based texture-based features are also used in classification. StarFocused has high energy (0.88) and homogeneity (0.98) as expected of its concentrated beam and Defined has higher contrast (2.05) of its sharper intensity transitions.

	Original IES image	**Light Region**	**Local Uniformity Map (U_{local})**
Display			

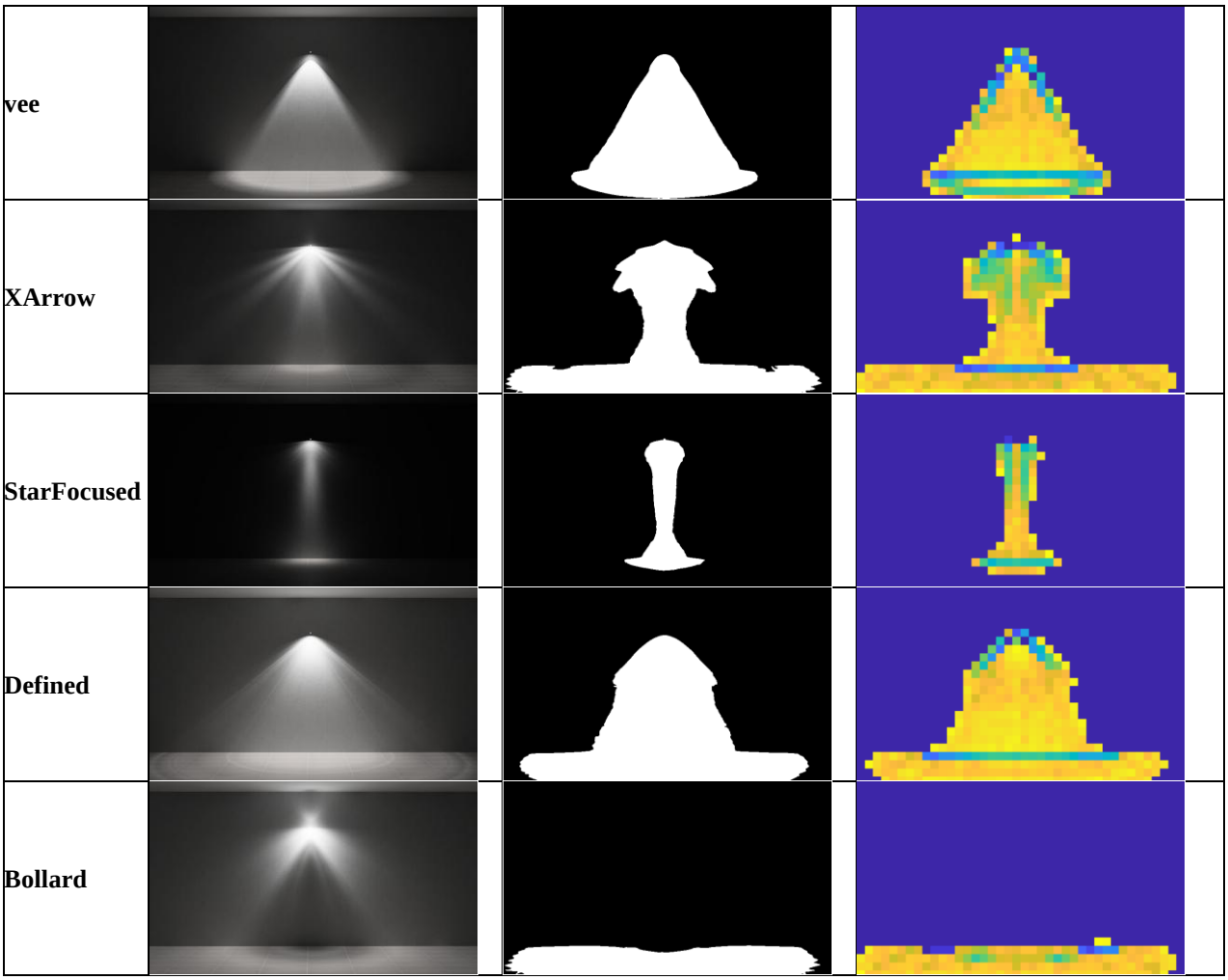
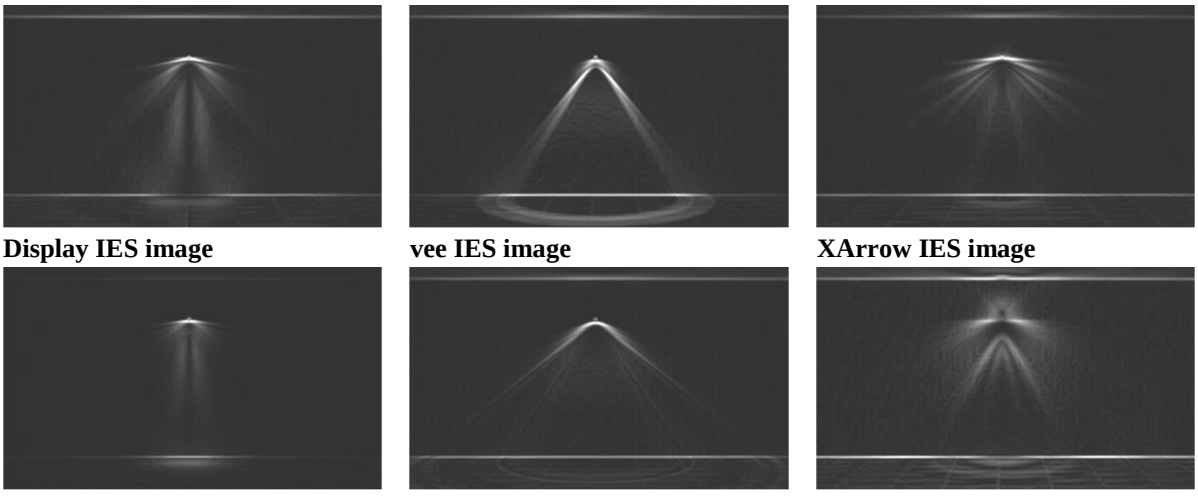
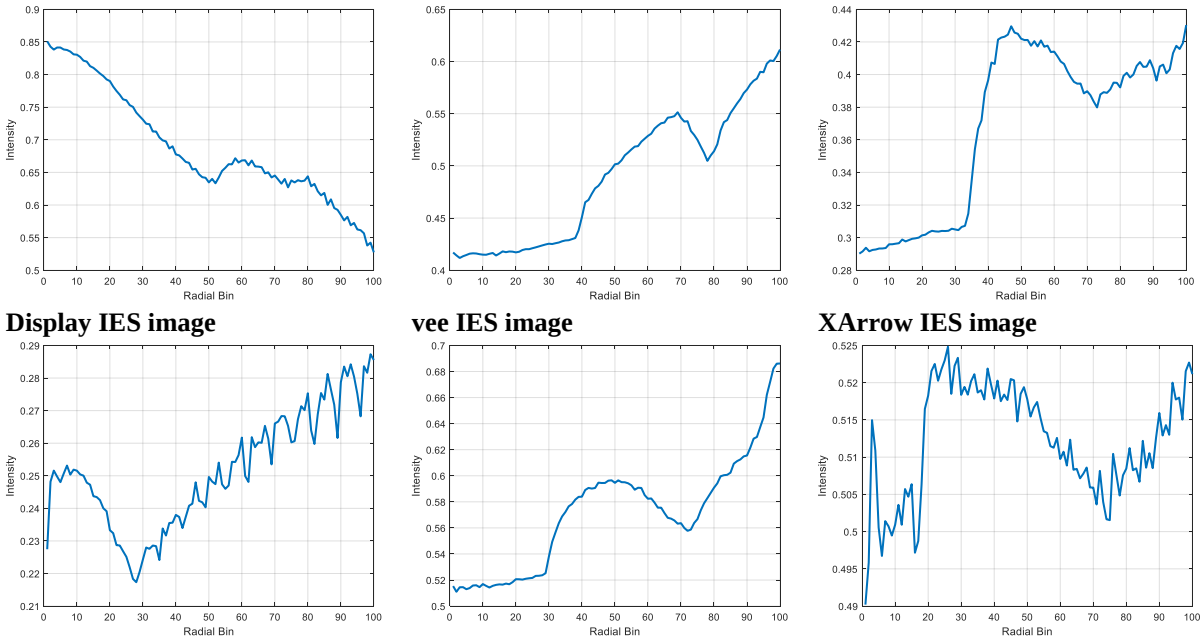


Fig (4) Illustration of the feature extraction process for six representative IES light patterns. Each column shows the original IES image, the segmented light region, and the local uniformity map (U_{local}). This visualization highlights the differences in beam spread, edge sharpness, and local uniformity across the tested distributions (Display, Vee, XArrow, Star Focused, Defined, Bollard).



Fig(5) Gradient Magnitude Map of six representative IES light patterns

To further illustrate the extracted descriptors, the following are figures illustrating radial intensity profile of different IES patterns of lights. These plots emphasize on intensity variation with radial distance which provides a visual comparison of distributions of focused and ambient beam distributions.



Display IES image **vee IES image** **XArrow IES image**

Star Focused IES image **Defined IES image** **Bollard IES image**

Fig(6) :Radial Intensity Profile of IES Light images

6. ADVANCED FEATURE VALUES ANALYSIS

In this section, an advanced descriptors derived out of the beam patterns are summarized comparatively. Every feature group introduces certain distinctive geometric, statistical and textural qualities useful in classification and analysis related to the specific application. These values are clustered into properly organized categories as displayed in the table below and this allows one to easily calculate discriminative parameters under different lighting conditions.

Table (2) Tabulated Overview of Advanced Feature Descriptors for Beam Classification

No.	Main Features	Statistical Shape Descriptors	Beam Characteristics Details
1.	Geometric and Spatial Features	Radius	Highest in Defined (189.77) and XArrow (172.90), indicating broader radial spread.
			Lowest in Star-Focused (85.18), consistent with its concentrated central beam.
		Center Shift	Extremely low in Bollard (20.31), suggesting strong central alignment.
			High in XArrow (224.34) and Display (222.08), reflecting off-center intensity distribution.
		Ellipticity	Bollard shows extreme ellipticity (11.31), indicating highly elongated beam shape.
			Star-Focused also elevated (3.62), while Vee remains nearly circular (1.06).
		Implication	Ellipticity and CenterShift are strong discriminators for classification, especially for Bollard and Star-Focused.
2.	Uniformity and Distribution	Uniformity (U_0)	Bollard (0.54) and XArrow (0.46) show high uniformity.
			Star-Focused (0.00) indicates complete lack of uniformity, consistent with its sharp central hotspot.
		Hotspot Density	Highest in Display (0.34) and Bollard (0.39), suggesting dense luminous clusters.
			Lowest in XArrow (0.19), reflecting dispersed peaks.
		Entropy	Display (7.12) highest entropy → complex distribution.
			Bollard lowest (5.96) → simpler, less varied pattern.
		Implication	Entropy and Uniformity provide complementary measures complexity vs. smoothness useful for anomaly detection.
3.	Statistical Shape Descriptors	Skewness	Strongly positive in XArrow (1.95) → asymmetric distribution with long tail.
			Negative in Bollard (-0.19) → intensity skewed toward lower values.
		Kurtosis	Very high in XArrow (6.41) and Star-Focused (4.39) → sharp peaks.
			Lower in Display (1.76) and Bollard (1.86) → flatter distributions.
		Implication	Skewness and Kurtosis highlight peaked vs. flat intensity profiles, critical for distinguishing XArrow and Star-Focused.
4.			Narrowest in Star-Focused (89) → concentrated beam.

No.	Main Features	Statistical Shape Descriptors	Beam Characteristics Details
	Beam Characteristics	**Beam Width Pixels**	Widest in Bollard (769) and Defined (614) → broad coverage.
		Beam Angle deg	Bollard widest angle (144.65°).
			Star-Focused narrowest (55.17°).
		Implication	Beam width and angle strongly correlate with application type (focused vs. ambient lighting).
5.	**Texture Features (GLCM)**	**GLCM-Contrast**	Highest in Defined (2.05) and Display (1.99) → sharper intensity transitions.
			Lowest in Star-Focused (0.49) → smoother texture.
		GLCM-Energy	Highest in Star-Focused (0.88) → highly ordered pattern.
			Lowest in Defined (0.48) → more complex texture.
		GLCM-Homogeneity	Highest in Star-Focused (0.98) → uniform texture.
			Lowest in Defined (0.93) → more irregularity.
		Implication	Texture descriptors (contrast, energy, homogeneity) provide strong signals for differentiating Star-Focused (smooth, uniform) from Defined (complex, irregular).
6.	**Intensity and Falloff**	**Max Intensity and Peak Intensity**	All normalized to 1.0 except Bollard (0.67), indicating weaker peak intensity.
		Falloff	Positive in Display (0.32) → gradual decline.
			Negative in Vee, XArrow, Defined → sharper drop-off.
		Implication	Falloff and peak intensity distinguish Bollard as a low intensity, ambient source.

Table (3) Qualitative Analysis of Each IES Image Profile

IES Image Patterns	Curve Characteristics	Distinctive Features	Implications for Classification
Display	Nearly flat curve with minor oscillations	Homogeneous distribution	Serves as a baseline or reference pattern
Vee	Sharp decline with a pronounced peak	Strong directionality	Indicates targeted illumination
XArrow	Multi-peaked curve	Irregular distribution	Represents complex, multi-directional lighting
Star-Focused	Central peak with rapid decay	Strong central focus	Easily distinguishable concentrated pattern
Defined	Stable, regular curve	Clear radial boundaries	Functions as a reference "well-defined" profile
Bollard	Gradual decline, no sharp peaks	Low-intensity ambient spread	Characteristic of diffuse, low-density lighting

All in all, the features that have been extracted present a strong foundation to machine learning classifiers. The algorithms (SVM and Random Forest) can utilize the high separation of both geometric and statistical features whereas neural networks (MLP) can make use of the texture descriptors to represent finer details. Besides, features like ellipticity and center shift are considered to be extreme deviations, which facilitates the detection of anomalies or faulty light patterns. The visual analysis in Figure (6) shows that there is diversity in the distribution of light on the tested patterns. Thin beams like StarFocused and XArrow are characterized by sharp gradients and low local uniformity whereas wide beams like Display and Bollard have smooth transitions and high variability in uniformity. It is worth noting that Bollard is characterized by extreme ellipticity and anomalous uniformity behavior which is in line with its classification as a possible outlier of the feature-based analysis. These plots validate the features being received and provide a hunch-proof of the classification and anomaly detection model.

To further explain the contrast point between the light patterns which are under the analysis, Figure X compares the entire distributions including the original IES image, the segmented light area, gradient magnitude map and local uniformity map (U_{local}). These pictures give the qualitative data to the numerical feature analysis of the differences in beam distribution, edge sharpness, and consistency. The key characteristics which occurred in all patterns can be outlined in the following way:

1. Display: Wide beam with smooth transitions; gradient map shows moderate edge sharpness, uniformity map indicates balanced distribution.
2. Vee: Wide beam but sharper edges compared to Display; gradient map highlights strong directional spread.

3. XArrow: Narrow beam with concentrated hotspots; gradient map reveals sharp transitions, uniformity map shows low local uniformity.
4. StarFocused: Very narrow, highly concentrated beam; uniformity map confirms extreme non-uniformity.
5. Defined: Balanced beam with clear edges; gradient map shows strong contrast, uniformity map indicates moderate uniformity.
6. Bollard: Extremely wide and elliptical beam; gradient map shows diffuse edges, uniformity map highlights anomalies consistent with outlier behavior.

7. THE GRADIENT MAGNITUDE MAP

A Gradient Magnitude map is an important analytical tool because it shows areas of rapid change in light intensity within a lighting pattern. It reveals the boundaries or edges within the light distribution, where the transition from bright to dark areas is most pronounced. If we apply this definition to the six lighting patterns (Display, Vee, X-Arrow, Star Focused, Defined, Bollard) discussed earlier, the observations can be listed as follows:

Table (4) Gradient Magnitude Analysis of Six IES Light Distribution Patterns

Pattern	The Gradient Map appearance	Visual implication
Display	Strong edges around the center	Shows concentrated light at a point with sharp transitions at the boundaries.
Vee	Gradient lines forming a V-shape	Reveals uneven transitions between the arms, explaining weak uniformity.
XArrow	Four intersecting axes with clear edges	Indicates multi-directional spread with unbalanced transition zones.
StarFocused	Bright center with strong radial edges	Highlights high central focus with rapid fall-off at the periphery.
Defined	Clear and well-structured boundaries	Reflects precise light distribution with relatively balanced transitions.
Bollard	Wide but weak edges	Shows broad ground-level spread with gradual transitions, suitable for coverage rather than uniformity.

8. RADIAL INTENSITY PROFILE ANALYSIS

More insight into the spatial distribution of light of different IES patterns is provided by the radial intensity profiles. Display image shows that the beam is comparatively wide and gradual decrease of intensity, which shows the curves of smooth transition between the center and outward. The Tree profile, however, is the one that has irregular variation, i.e. there was no homogeneity in the distribution of light and there was a change of directions. The XArrow pattern has the central peak steep and then steep as one will expect in a narrow and concentrated beam. Similarly, the StarFocused profile depicts an even steeper peak, which confirms its highly focused behavior of spotlight. Defined image possesses a balanced profile with sharp edges and medium distribution which stresses the ordered beam character. The Bollard profile is the final profile and is flatter and more elongated which is very wide and elliptical with diffuse edges.

These results are correlated with the numerical analysis of features in that narrow beams (StarFocused, XArrow) have sharp intensity peaks and low uniformity, and wide beams (Display, Bollard) have fewer sharp transitions and more variability. The aberrate Ness of Bollard specifically coincides with the fact that it is a possible outlier in the anomaly detection.

9. DISCUSSION

The higher photometric measurement of the 6 light pattern patterns of IES (Display, Vee, XArrow, StarFocused, Defined, and Bollard) is a unified and holistic-based luminous behavior methodology and can be applied to help classify and detect anomalies AI-based. The research is able to integrate image-based maps, numerical descriptors and radial intensity profiles to form a multi-dimensional approach that is more intuitively sound and strong.

Defined and Bollard have wider angles of beam and a higher radius, geometrical in nature meaning that the light distribution is wide contrary to StarFocused that has a small radius and narrow beam angle. The CenterShift and Ellipticity values also show the uniqueness of Bollard that possesses very minimal central displacement and high ellipticity, which presupposes the non-circular and elongated shape of the beam.

Discriminative power is also obtained by measures of uniformity and radial symmetry. Bollard is also as uniform and homogeneous as possible meaning that the light field is homogeneous. Star on the other hand is nearly devoid of uniformity and that is why it is the sharpest central hot spot. Vee, XArrow and Defined falloff values are negative which show gradual decrease in intensity but Display falloff values are positive which mean gradual transitions.

The statistical descriptors used to indicate the difference in the complexity of distribution are entropy, skewness, and kurtosis. Maximum entropy is displayed, hence, there is an abundance and intricate distribution of light. XArrow is extremely skewed and kurtosed and therefore is asymmetrical and whose variation is heavily skewed. Conversely, Bollard was the only pattern that has negative skewness meaning that it is oriented to low intensity.

The support of these observations is supported by features of the texture due to the GLCM analysis. StarFocused possesses an energy and homogeneity optimality, which complies with its simple and centralized structure. Defined has the largest difference, and the severe changes of intensity throughout the beam. The fact that the correlation values are high in all the patterns indicates that the structural regularity is high and this is beneficial to machine learning models.

These results are confirmed by radial intensity profiles that demonstrate the way luminous intensity fades away. Display and Vee have gradual falloff curves, which are in line with extensive coverage. XArrow and XTArrow show steeper falls, which are directional beams. StarFocused has a sharp central peak with a sharp attenuation, whereas Bollard has a lower maximum intensity but a longer beam width which is in accordance with its diffuse lighting purpose.

All these findings support the strength of the features that are extracted in the visual, statistical, and radial domains. Combination of geometric, statistical and texture-based descriptors offers a holistic approach to AI-based classification and anomaly detection, whereas the similarity of results in various perspectives reinforces the effectiveness of the offered approach.

10. CONCLUSION

This work introduced an AI-based system of IES light patterns classification and anomalies detection based on image-based photometric characteristics. The system was able to distinguish various patterns of light including narrow beams, wide beams and non-uniform patterns by deriving a set of comprehensive geometric, statistical, and texture features. The flexibility in characteristics like beam angle, uniformity, ellipticity and center shift gave a good discriminative value to machine learning classifiers, whereas texture measures gave better capabilities of detecting finer changes in light distribution. The high-level photometric feature analysis of the six IES lighting patterns (Display, Vee, XArrow, StarFocused, Defined, and Bollard) disclosed that there is clear geometry, statistical, and textural-based traits which are very useful in AI-based classification and anomaly detection. Defined and Bollard were distributed geometrically in general, and StarFocused was narrow and concentrated beam wise. CenterShift and Ellipticity introduced elongation of Bollard and the homogeneity of its measures in uniformity and radial symmetry were compared to the spikey hot spot of StarFocused. The behaviors of radial falloff also provided information on discrimination patterns that were better, and Vee, XArrow and Defined decreased gradually, in contrast to these transitions in Display being so abrupt. These differences were supported by the statistical descriptors: Display had high entropy, XArrow extreme skew and kurtosis and Bollard was the one that had negative skew. The results were complemented with texture based GLCM features which have StarFocused features and high energy and homogeneity, defined features which have high contrast, and always good value of correlation with all patterns connotations of structural regularity. All these multi-dimensional descriptors testified to the strength of the photometric features analysis that is interpretable and discriminative in automated classification as well as detection of the anomaly of the lighting systems. Besides, the combination of the geometric [12,13], statistical, gradient-based, uniformity-based, texture-based (GLCM) and the radial intensity features offered a combined and trustworthy model of the analysis of the various IES lighting patterns. Each kind of image possessed its own photometric fingerprint and once they were converted to quantitative features, such as radius, entropy, skewness, kurtosis, and GLCM features, they became easier to understand and more powerful in terms of classification using AI. SVM, random forests, KNN and MLP classifier have successfully employed such features to provide the right categorization and drastic deviations in geometric and statistical measurements as far as assist in diagnosis of anomalies. Along with the detection of anomalies, the proposed framework promotes such practical applications as automated quality checks in luminaire manufacturing, smart and architectural lighting design, and the development of standardized datasets which can be used in machine learning. Future studies need to focus on augmenting the dataset with more light patterns and to add the corresponding descriptors to the deep learning models (e.g., convolutional neural networks, autoencoders) and apply the framework to study its effectiveness on the real-life lighting systems. Such extensions would render this research more applicable and contribute to the creation of smart lighting technologies. As a rule, the findings verify the efficiency of the advanced photometric features analysis as a comprehensive and reliable tool of AI-based evaluation, classification, and detection of aberration in the light systems.

REFERENCES

1) Carrington, K. D. (2006). A photometric characterization methodology for daylighting fixtures. North Carolina State University.
2) Giroux, J., Dastjerdi, M. R. K., Hold-Geoffroy, Y., Vazquez-Corral, J., & Lalonde, J. F. (2024). Towards a perceptual evaluation framework for lighting estimation. In *Proceedings of the IEEE/CVF Conference on Computer Vision and Pattern Recognition* (pp. 4410-4419).

3) Zhan, F., Zhang, C., Yu, Y., Chang, Y., Lu, S., Ma, F., & Xie, X. (2021, May). Emlight: Lighting estimation via spherical distribution approximation. In Proceedings of the AAAI Conference on Artificial Intelligence (Vol. 35, No. 4, pp. 3287-3295).
4) Tusher, M. B. U., Akash, S. K., & Showmik, A. I. (2025). Anomaly Detection Using Computer Vision: A Comparative Analysis of Class Distinction and Performance Metrics. *arXiv preprint arXiv:2503.19100*.
5) Singh, K., & Parihar, A. S. (2024). Illumination estimation for nature preserving low-light image enhancement. *The Visual Computer*, *40*(1), 121-136.
6) Al-khafaji K H. Regarding The Security of Discrete Fractional Fourier Transform in Color Image Encryption and Decryption. Al-Harf Journal. 2026; Feb 25 (1): 34-44.
7) Abdalla, M., Javed, S., Al Radi, M., Ulhaq, A., & Werghi, N. (2025). Video anomaly detection in 10 years: A survey and outlook. *Neural Computing and Applications*, 1-44.
8) Berkowitz, C., Carver, J., Hirschl, R., & Varma, S. (Eds.). (2024). *Advances in Pediatrics, 2024, E-Book* (Vol. 71, No. 1). Elsevier Health Sciences.
9) Shukla, V., Shukla, A., SK, S. P., & Shukla, S. (2025). A systematic survey: role of deep learning-based image anomaly detection in industrial inspection contexts. *Frontiers in Robotics and AI*, *12*, 1554196.
10) Bellia, L., Musto, M., & Spada, G. (2011). Illuminance measurements through HDR imaging photometry in scholastic environment. *Energy and buildings*, *43*(10), 2843-2849.
11) Standard, B. (2011). Light and lighting: Lighting of work places: Part 1: Indoor work places. Indoor work places.
12) Chauhan, B. V., Verma, S., Rahman, B. A., & Wyche, K. P. (2025). Deep learning in airborne particulate matter sensing and surface plasmon resonance for environmental monitoring. *Atmosphere*, *16*(4), 359.
13) Humeau-Heurtier, A. (2019). Texture feature extraction methods: A survey. IEEE access, 7, 8975-9000.